


COMMENTARY

Flow and shortcuts along the *Shaker* Kv channel slow inactivation gating cycle

 Valerie Abigail Nirenberg and Ofer Yifrach 

Slow inactivation gating in Kv channels natively or artificially lacking the fast inactivation “ball and chain” segment is usually described by a simple four-state gating cycle describing the dependence of one gate opening on the conformational state of the second. In the current issue of the *Journal of General Physiology*, Szanto et al. address flow along the gating cycle of the *Shaker*-IR channel during the onset of slow inactivation at negative membrane potentials and the consequences of locking open inactivated channels on recovery from slow inactivation. The authors demonstrated that the onset of slow inactivation in the *Shaker*-IR Kv channel occurs through the open state at either negative or positive voltages and that OI–CI transition is mandatory for recovery from slow inactivation. The results provide essential missing evidence that contribute to more complete understanding of *Shaker* channel slow-inactivation gating.

Voltage-dependent potassium ion currents through the membrane play fundamental roles in generating and shaping action potentials, as well as in determining their conductance properties, frequency, and firing modes (Jan and Jan, 2012; Bean, 2007; Zeberg et al., 2010). Such potassium currents are regulated in both spatial and temporal dimensions, as respectively determined by the clustering (Nirenberg and Yifrach, 2020) and gating mechanisms of Kv channel proteins (Yellen, 1998), through which such currents pass. Three primary gates along the ion conduction pore domain of Kv channels control the timing and amplitude of current flow through the channel: the activation gate (A) and the fast (N-type) and slow (C-type) inactivation gates (I_{O}^{fast} and I_{O}^{slow} , respectively). These gates undergo structural changes between open (O) and closed (C) states to allow or block K^{+} ion flow through the channel. Taking a reductionist view of Kv channel gating, and assuming that the inactivation “ball” can only “sneak” into its receptor site upon activation gate opening, six distinct but connected gating states are possible for a Kv channel, of which only one is conductive ($A_{O}I_{O}^{fast}I_{O}^{slow}$, Fig. 1 A). This thermodynamic view allows for addressing of the coupling between the activation and slow inactivation gates (left cycle) and between the two, fast and slow, inactivation mechanisms of the channel (right cycle). This Kv

channel gating scheme can be simplified by assuming a Kv channel natively or artificially (ΔI or IR) lacking the fast inactivation ball and chain N-terminal module (Fig. 1 B; Hoshi et al., 1991). In this issue of the *Journal of General Physiology*, Szanto et al. (2020) studied slow inactivation gating in the prototypical *Shaker*- ΔI Kv channel using the “duo modal” gating mechanism described in Fig. 1 B (Yellen, 1998; Panyi and Deutsch, 2006; Cuello et al., 2017) to address flow and shortcuts along the cycle during onset and recovery from slow inactivation at negative membrane potentials. Their results, obtained through an elegant experimental design, provide essential missing evidence that contributes to a more complete understanding of *Shaker* channel slow inactivation gating.

Initially, the authors asked whether the sequence of gating transitions leading to entry into and recovery from slow inactivation (Fig. 1 B) occurs along the same path at both extreme depolarizing and hyperpolarizing potentials. This may seem to be a trivial question at first. However, since voltage affects the stability of the different gating states along the cycle to different extents (and hence, the probability of the different gating transitions), a distinct slow inactivation gating sequence could well occur at very negative voltages, possibly through the closed channel state (i.e., the C–CI transition). The possibility of closed-state inactivation seems reasonable, considering the authors’ observation that steady-state slow inactivation in the *Shaker*- ΔI channel seems to occur even at hyperpolarizing voltages where no detectable activation was noted (see Fig. 2 in Szanto et al., 2020). To discern whether slow inactivation of the *Shaker*- ΔI channel at negative voltages occurs through the closed or open state, given how minute K^{+} currents traverse the channel in this voltage range, a sensitive quantitative handle to monitor the open state is needed. For this, the authors used the T449A;V474C double-mutant *Shaker*- ΔI channel that accelerates slow inactivation to a reasonable rate during recordings (T449A) (Hoshi and Armstrong, 2013) and which reacts with Cd^{2+} ions through cysteine-474 only in the open state (Liu et al., 1997; Panyi and Deutsch, 2006). Cd^{2+} -binding blocks K^{+} currents through the channel in a manner proportional to the probability

Department of Life Sciences and the Zlotowski Center for Neurosciences, Ben-Gurion University of the Negev, Beer Sheva, Israel.

Correspondence to Ofer Yifrach: ofery@bgu.ac.il.

© 2020 Nirenberg and Yifrach. This article is distributed under the terms of an Attribution–Noncommercial–Share Alike–No Mirror Sites license for the first six months after the publication date (see <http://www.rupress.org/terms/>). After six months it is available under a Creative Commons License (Attribution–Noncommercial–Share Alike 4.0 International license, as described at <https://creativecommons.org/licenses/by-nc-sa/4.0/>).

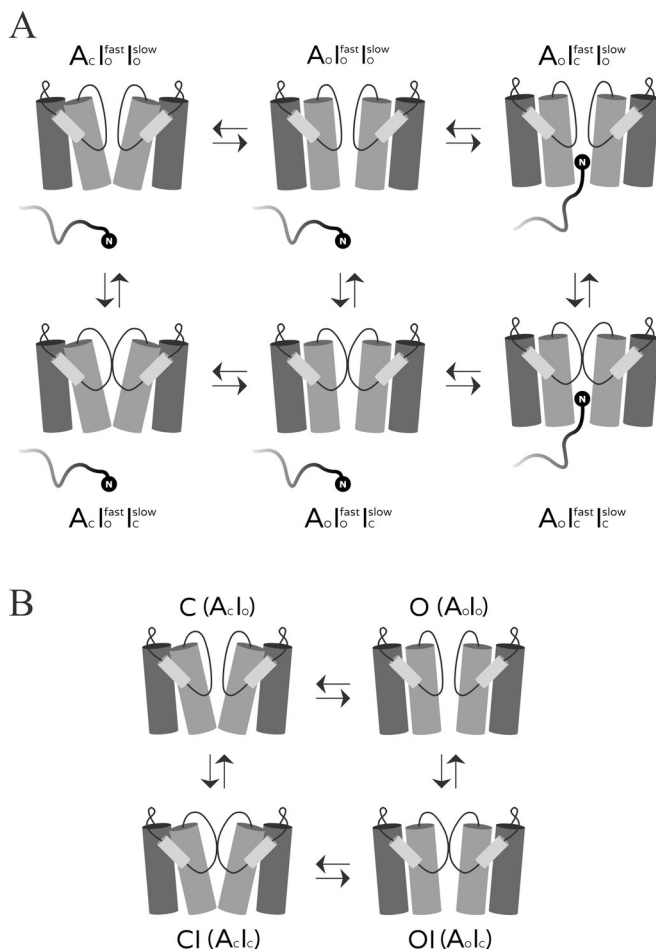


Figure 1. A reductionist view of *Shaker* Kv channel gating. (A) A simplistic gating scheme for a Kv channel with its three activation (A), fast inactivation (I^{fast}), and slow inactivation (I^{slow}) gates, corresponding to the S6 bundle crossing, the receptor site of the “chain”-attached ball element in the inner pore cavity, and the selectivity filter element, respectively, each undergoing a conformational transition between closed (C) and open (O) states. In this simplistic gating construct, each thermodynamic square corresponds to a context-dependent cycle that may serve to evaluate how the opening or closing of one gate depends on the conformational state of the other gate. Comparison of the ratio of equilibrium constants for any two parallel transitions would thus provide a quantitative assessment of the degree of coupling between the gates being compared. (B) A simplified cycle that describes the activation and slow inactivation gating of a *Shaker* Kv channel lacking the fast (N-type) ball and chain inactivation module (see also Fig. 1 in Szanto et al., 2020). The four states are designated C, O, OI, and CI, as commonly done, with the respective general designations given in parenthesis. For simplicity, the gating pathways described in all panels are portrayed by taking the reductionist view, whereby each gating state in a cycle probably represents a composite state.

of the channel being open (del Camino and Yellen, 2001). The characteristic steady-state activation and slow inactivation gating parameters of this mutant are comparable to those of the WT channel (see Fig. 2 in Szanto et al., 2020).

The authors devised an elegant three-pulse protocol and used inside-out patch clamp electrophysiological recordings to evaluate the pathway for onset of slow inactivation in the *Shaker*- Δ I T449A;V474C channel at negative membrane potentials (Fig. 2 A; see also Fig. 3 A in Szanto et al., 2020). The authors evaluated the

peak current amplitude (I_2) at a depolarizing voltage of +50 mV (P2) following a long -90-mV holding interval (H2) and in the presence of Cd^{2+} , relative to two identical peak current amplitudes (I_1 and I_3) obtained upon a -120 to +50 mV pulse, with one preceding the second pulse (P1) and the other (P3) following P2. The law of mass action along the characteristic gating scheme for the *Shaker*- Δ I channel (Fig. 1 B) serves to clarify the rationale behind this protocol in revealing whether the onset of slow inactivation at negative potentials passes through the closed or open state (Fig. 2 A). Peak current under the different conditions reflects the availability of channels in the closed state (C or $A_c I_o$) that are prone to be open upon strong depolarization (the O or $A_o I_o$ state). Indirectly, it further reports on the presence of silent, noncurrent contributing states, like the CI ($A_c I_c$) or OI ($A_o I_c$) channel states available at each condition before pulse onset. For example, at the -120-mV holding voltage before P1 (Fig. 2 A, segment H1), all channels within the membrane patch are assumed to be in the closed state (C), yet are open upon strong depolarization to +50 mV, thus reflecting the maximal current amplitude possible. At the -90-mV holding potential and in the presence of Cd^{2+} ions, the majority of channels will indeed remain in the closed state; however, the CI and OI states (or their Cd^{2+} -bound states) could also be populated, depending on whether, at this voltage, closed channels are prone to inactivate, either directly, through the C-CI transition (Fig. 2 A; blue transition), or indirectly, through the open channel state (C \rightarrow O \rightarrow OI \rightarrow CI; Fig. 2 A; red transition sequence). At this middle pulse, and in either case, I_2 is likely smaller than I_1 . The role of the third pulse then is to distinguish between the two possibilities. If at -90 mV and in the presence Cd^{2+} ions inactivation occurs solely through the closed state, then I_3 should be equal to I_1 , as all channels are in the closed state before the third +50 mV voltage shift (blue box under H3). Whether or not Cd^{2+} is present in the bath solution during H2 does not matter, as Cd^{2+} can block potassium currents only when the channel is open (Liu et al., 1997). If, however, at this voltage, slow inactivation occurs through the open channel state and all available open channels are modified by Cd^{2+} , then I_3 should be smaller than I_1 yet equal to I_2 ($I_1 > I_3 = I_2$). I_3 would be lower than I_1 because, given the long (20 s) -90-mV holding interval (segment H2), Cd^{2+} would bind to all available open channels and block their ion conduction pathways, making this channel fraction transparent in electrophysiological recordings, irrespective of whether the bound channel is open, closed, or in the inactivated state. At the -120-mV holding interval before the third pulse (segment H3), this fraction of modified channels would assume the closed state (red box under H3) and not contribute to observed peak current during the onset of the third pulse, thus rendering $I_3 = I_2$.

These considerations are summarized by the quantity of recovered current fraction (RCF) defined by the authors as $\text{RCF} = (I_3 - I_2) / (I_1 - I_2)$ (see Fig. 3 in Szanto et al., 2020). This quantity elegantly demonstrates how closed- or open-state inactivation at negative potentials can be discriminated using the three-pulse protocol. RCF equals 1 when slow inactivation at negative potential occurs solely through the closed state, in which case $I_1 = I_3$. At the other extreme, an RCF of 0 reflects the case where slow inactivation occurs predominantly through the open state and

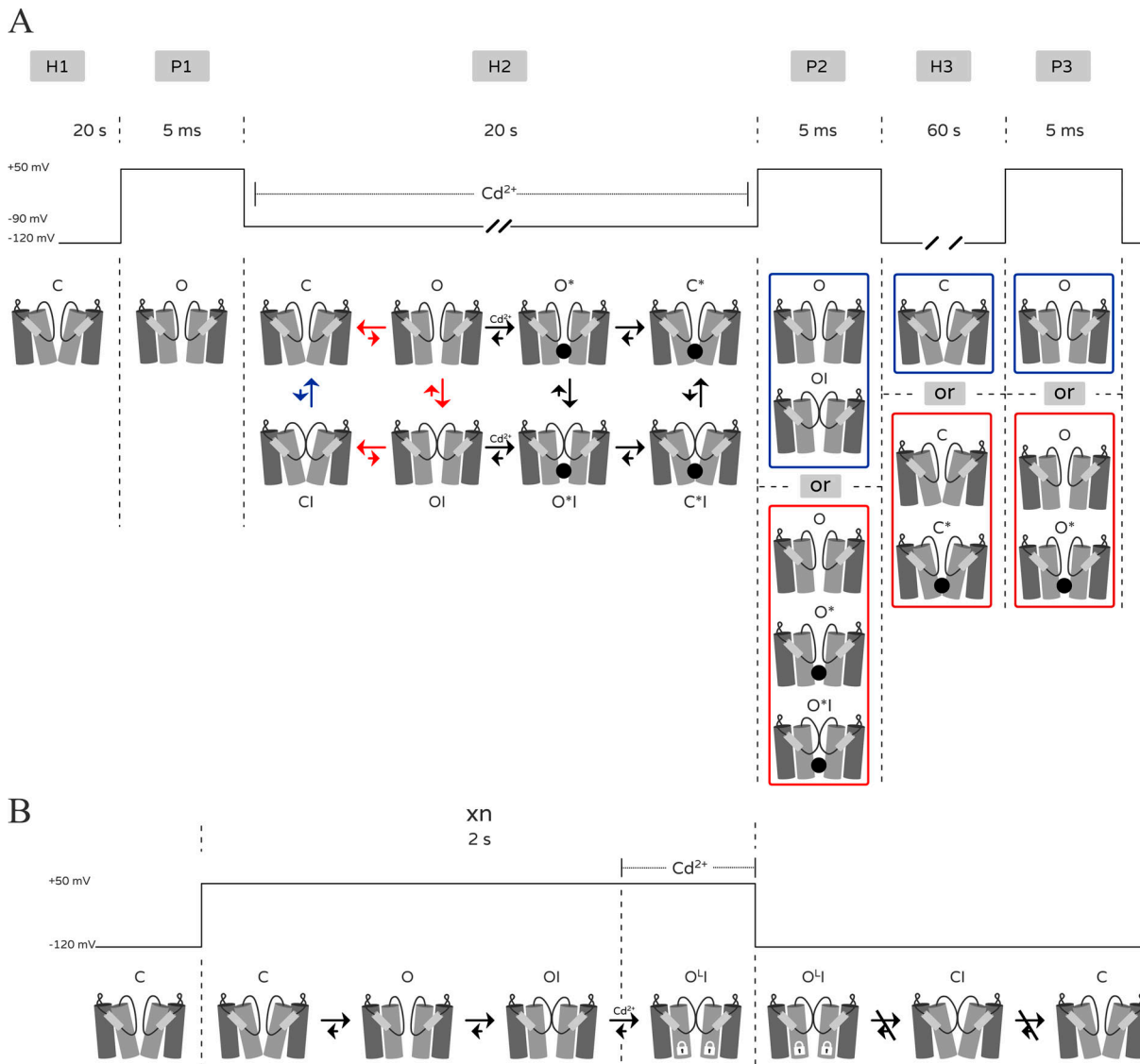


Figure 2. Flow and shortcuts along the *Shaker* Kv channel slow inactivation gating cycle. (A) Depiction of the three-pulse protocol devised by Szanto et al. (2020) to assess whether the onset of slow inactivation in the *Shaker-ΔI* Kv T449A;V474C double-mutant channel at negative membrane potentials occurs through the open or closed states. The voltage and duration of each holding (H) or pulse (P) step is indicated, as is when Cd²⁺ ions (black circle) were applied (solid line above segment H2). Below each H or P segment, the probable channel states are indicated, as principally and qualitatively determined using the law of mass action along the slow inactivation gating cycle of the *Shaker-ΔI* Kv channel (Fig. 1 B). The red or blue gating sequences along the cycle shown below the -90-mV holding segment (H2) correspond to the onset of slow inactivation through the open or closed state, respectively. Cd²⁺-binding steps or gating transitions among Cd²⁺-bound states are indicated by black arrows. Channel gating states in which Cd²⁺ is bound are indicated by an asterisk. The magnitudes of forward and backward rate constants, determining the prevalence of each state, are qualitatively indicated by the length of each arrow. Note that the timescales of the different holding intervals are not scaled. To monitor whether Cd²⁺ modification depends on the probability of the channel being open, the protocol was repeated, setting the H2 holding voltage to either -80 or -70 mV. **(B)** The protocol used by Szanto et al. (2020) to investigate whether the OI-CI gating transition of the *Shaker-ΔI* Kv T449A;V476C double-mutant channel is mandatory for recovery from slow inactivation. Locking the channel in the OI state is achieved by applying Cd²⁺ toward the end of the pulse protocol (solid line). The creation of a Cd²⁺-mediated inter-subunit metal ion cross-bridge locks the channel open (O-I), thus preventing the OI-CI transition and providing a shortcut for flow along the slow inactivation gating cycle (see text for further details). *n* represents the multiple times the protocol was repeated (represented by the letter *x*).

assuming all channels open at -90 mV are Cd²⁺-bound ($I_3 = I_2$). RCF values close to 0 ($0 < RCF \ll 1$) reflect slow inactivation through the open state when not all open channels at -90 mV are Cd²⁺-modified. Here, $I_1 > I_3 > I_2$, since the pull of CI or OI non-modified states populated before the second pulse (the -90-mV H2 segment) can recover to the closed state when the holding potential is restored to -120 mV.

Following steady-state characterization of the activation and slow inactivation gating properties of the *Shaker-ΔI* T449A;V474C channel (see Fig. 2 in Szanto et al., 2020) and proper controls (see Fig. 4 in Szanto et al., 2020), the authors showed that at a negative holding potential (-70, -80, or -90 mV) applied in H2 before the middle P2 test pulse (in the presence of 20 μM Cd²⁺ in the bath solution), RCF values between 0.1 and 0.4

were obtained for the double-mutant channel (see Fig. 5 in Szanto et al., 2020). Furthermore, the RCF is both voltage- and $[Cd^{2+}]$ -dependent with increased depolarization or increased Cd^{2+} concentrations, resulting in lower, close to 0 values (see Fig. 5 C in Szanto et al., 2020). Lastly, whether Cd^{2+} modification of the double mutant at a given negative voltage (e.g., -90 mV) achieved through one long exposure or multiple cycles of short exposures yields identical results with respect to entry into slow inactivation (see Fig. 6 in Szanto et al., 2020). Given the close to 0 RCF values obtained, the results revealed that the onset of slow inactivation in the *Shaker-ΔI* T449A;V474C channel at negative membrane potentials occurs through the open channel state. Thus, despite the lack of observable activation currents at -90 mV (see Fig. 2 in Szanto et al., 2020), the pathway for onset of slow inactivation at negative voltage passes through the $C \rightarrow O \rightarrow OI$ gating sequence, as observed at depolarizing voltages (Panyi and Deutsch, 2006; Kurata and Fedida, 2006). Here, however, the sequence of steps continues onto the CI state, since at -90 mV the lower activation gate is predominantly stabilized in its closed state. Thus, unlike other *Shaker* Kv channel mutants that exhibit dramatically altered gating properties, no evidence for direct $C \rightarrow CI$ closed-state slow inactivation gating transition was found for the WT-like double-mutant channel studied by Szanto et al. (2020).

To investigate whether $OI \rightarrow CI$ transition is mandatory for *Shaker-ΔI* recovery from slow inactivation (Panyi and Deutsch, 2006; Kurata and Fedida, 2006), the authors used the T449A;V476C double mutant. Previous results indicated that the V476C mutant enables locking the activation gate of the channel in the open state, even at negative membrane potentials, by forming an inter-subunit Cd^{2+} -mediated metal cross-bridge with H486 at neutral pH (~ 7.4 ; Holmgren et al., 1998; Webster et al., 2004). This *Shaker-ΔI* T449A;V476C double mutant is thus suitable for realizing the pathway for channel recovery from slow inactivation, and in particular, the role of the $OI \rightarrow CI$ transition in this process. Following biophysical characterization of this mutant channel expressed in HEK cells using an inside-out patch-clamp configuration (see Fig. S3 in Szanto et al., 2020), the authors evaluated the consequences of locking the activation gate of inactivated channel (OI) open on recovery from inactivation (Fig. 2 B). Onset and recovery from slow inactivation in the double mutant were induced by a 2-s-long square pulse from -120 to $+50$ mV and back. Control experiments performed in the absence of Cd^{2+} ions revealed a similar value for the peak current when the protocol was repeated every 60 s several times while holding the potential at -120 mV (see Fig. 7 A in Szanto et al., 2020). Thus, under these conditions, the *Shaker-ΔI* T449A;V476C channel fully recovers from slow inactivation. When, however, Cd^{2+} was applied for a short time toward the end of the depolarizing pulse (i.e., when the channel is deep in the OI state), and the pulse was repeated every 60 s, as before, an exponential decrease in the peak current was observed as function of cumulative Cd^{2+} exposure time (see Fig. 8 in Szanto et al., 2020). This reduction in peak current amplitude was completely abolished when the experiment was repeated in acidic bath solution (pH 5.3, but with Cd^{2+} ions; see Fig. 9 in Szanto et al., 2020), a condition which facilitates H486 protonation and

prevents metal cross-bridge formation with C476 (Webster et al., 2004). Thus, metal bridge-mediated locking down of the *Shaker* channel in the OI state (OI^L) prevents $OI \rightarrow CI$ transition and completely abolishes channel recovery from slow inactivation. This transition occurs very fast in the WT channel upon membrane repolarization and is mandatory for recovery to the closed state, where the slow inactivation gate is open ($CI \rightarrow C$ transition, induced by sufficiently negative and prolonged repolarization; Panyi and Deutsch, 2006). This locked-open inactivated channel further prevents $OI \rightarrow O$ transition, a manifestation of the strong negative coupling between the lower activation and upper slow inactivation gates, as manifested by channel-gating states with opposite gate configurations (e.g., the $A_{CI} [C]$ or $A_{OI} [OI]$ states; Panyi and Deutsch, 2006; Ben-Abu et al., 2009). These results thus provide clearcut evidence that recovery in the *Shaker-ΔI* channel occurs through the $OI \rightarrow CI \rightarrow C$ transition sequence, thus completing flow along the *Shaker-ΔI* slow inactivation gating cycle.

To summarize, the study by Szanto et al. (2020) teaches that directionality and flow along the slow inactivation gating cycle of the *Shaker-ΔI* Kv channel (Fig. 1 B) is preserved during onset and recovery from slow inactivation at both positive and negative potentials. Onset of slow inactivation is achieved only following activation gate opening. No detectable closed-state inactivation occurs for the *Shaker* channel, even at negative membrane potentials. Furthermore, shortcircuiting the gating cycle of the *Shaker* channel by locking the channel in the inactivated open state (OI) prevents forward flow along the cycle, resulting in an inability of the channel to recover from slow inactivation and returning to the closed starting state. These results add to previous seminal reports on slow inactivation in this prototypical channel (Panyi and Deutsch, 2006; Kurata and Fedida, 2006) and, together with the wealth of structural, functional, and dynamics data recently obtained on the intensively studied KcsA model channel (Cuello et al., 2010a, 2010b; Cuello et al., 2017; Labro et al., 2018), provide coherent atomic- and mechanistic-level understanding of slow inactivation gating in potassium channels.

Acknowledgments

Christopher J. Lingle served as editor.

This research was supported by the Israel Science Foundation (grant 294/16 to O. Yifrach).

The authors declare no competing financial interests.

References

- Bean, B.P.. 2007. The action potential in mammalian central neurons. *Nat. Rev. Neurosci.* 8:451–465. <https://doi.org/10.1038/nrn2148>
- Ben-Abu, Y., Y. Zhou, N. Zilberberg, and O. Yifrach. 2009. Inverse coupling in leak and voltage-activated K^+ channel gates underlies distinct roles in electrical signaling. *Nat. Struct. Mol. Biol.* 16:71–79. <https://doi.org/10.1038/nsmb.1525>
- Cuello, L.G., V. Jogini, D.M. Cortes, A.C. Pan, D.G. Gagnon, O. Dalmas, J.F. Cordero-Morales, S. Chakrapani, B. Roux, and E. Perozo. 2010a. Structural basis for the coupling between activation and inactivation gates in $K(+)$ channels. *Nature.* 466:272–275. <https://doi.org/10.1038/nature09136>

- Cuello, L.G., V. Jogini, D.M. Cortes, and E. Perozo. 2010b. Structural mechanism of C-type inactivation in K(+) channels. *Nature*. 466:203–208. <https://doi.org/10.1038/nature09153>
- Cuello, L.G., D.M. Cortes, and E. Perozo. 2017. The gating cycle of a K⁺ channel at atomic resolution. *eLife*. 6. e28032. <https://doi.org/10.7554/eLife.28032>
- del Camino, D., and G. Yellen. 2001. Tight steric closure at the intracellular activation gate of a voltage-gated K(+) channel. *Neuron*. 32:649–656. [https://doi.org/10.1016/S0896-6273\(01\)00487-1](https://doi.org/10.1016/S0896-6273(01)00487-1)
- Holmgren, M., K.S. Shin, and G. Yellen. 1998. The activation gate of a voltage-gated K⁺ channel can be trapped in the open state by an intersubunit metal bridge. *Neuron*. 21:617–621. [https://doi.org/10.1016/S0896-6273\(00\)80571-1](https://doi.org/10.1016/S0896-6273(00)80571-1)
- Hoshi, T., and C.M. Armstrong. 2013. C-type inactivation of voltage-gated K⁺ channels: pore constriction or dilation? *J. Gen. Physiol.* 141:151–160. <https://doi.org/10.1085/jgp.201210888>
- Hoshi, T., W.N. Zagotta, and R.W. Aldrich. 1991. Two types of inactivation in Shaker K⁺ channels: effects of alterations in the carboxy-terminal region. *Neuron*. 7:547–556. [https://doi.org/10.1016/0896-6273\(91\)90367-9](https://doi.org/10.1016/0896-6273(91)90367-9)
- Jan, L.Y., and Y.N. Jan. 2012. Voltage-gated potassium channels and the diversity of electrical signalling. *J. Physiol.* 590:2591–2599. <https://doi.org/10.1113/jphysiol.2011.224212>
- Kurata, H.T., and D. Fedida. 2006. A structural interpretation of voltage-gated potassium channel inactivation. *Prog. Biophys. Mol. Biol.* 92:185–208. <https://doi.org/10.1016/j.pbiomolbio.2005.10.001>
- Labro, A.J., D.M. Cortes, C. Tilegenova, and L.G. Cuello. 2018. Inverted allosteric coupling between activation and inactivation gates in K⁺ channels. *Proc. Natl. Acad. Sci. USA*. 115:5426–5431. <https://doi.org/10.1073/pnas.1800559115>
- Liu, Y., M. Holmgren, M.E. Jurman, and G. Yellen. 1997. Gated access to the pore of a voltage-dependent K⁺ channel. *Neuron*. 19:175–184. [https://doi.org/10.1016/S0896-6273\(00\)80357-8](https://doi.org/10.1016/S0896-6273(00)80357-8)
- Nirenberg, V.A., and O. Yifrach. 2020. Bridging the molecular-cellular gap in understanding ion channel clustering. *Front. Pharmacol.* 10:1644. <https://doi.org/10.3389/fphar.2019.01644>
- Panyi, G., and C. Deutsch. 2006. Cross talk between activation and slow inactivation gates of Shaker potassium channels. *J. Gen. Physiol.* 128:547–559. <https://doi.org/10.1085/jgp.200609644>
- Szanto, T.G., F. Zakany, F. Papp, Z. Varga, C.J. Deutsch, and G. Panyi. 2020. The activation gate controls steady-state inactivation and recovery from inactivation in Shaker. *J. Gen. Physiol.* 152. e202012591. <https://doi.org/10.1085/jgp.202012591>
- Webster, S.M., D. Del Camino, J.P. Dekker, and G. Yellen. 2004. Intracellular gate opening in Shaker K⁺ channels defined by high-affinity metal bridges. *Nature*. 428:864–868. <https://doi.org/10.1038/nature02468>
- Yellen, G.. 1998. The moving parts of voltage-gated ion channels. *Q. Rev. Biophys.* 31:239–295. <https://doi.org/10.1017/S0033583598003448>
- Zeberg, H., C. Blomberg, and P. Arhem. 2010. Ion channel density regulates switches between regular and fast spiking in soma but not in axons. *PLOS Comput. Biol.* 6. e1000753. <https://doi.org/10.1371/journal.pcbi.1000753>